



## Article

# Intra-Seasonal Variability of Sea Level on the Southwestern Bering Sea Shelf and Its Impact on the East Kamchatka and East Sakhalin Currents

Andrey Andreev

V.I. Il'ichev Pacific Oceanological Institute, 690041 Vladivostok, Russia; andreev@poi.dvo.ru

**Abstract:** The East Kamchatka and East Sakhalin Currents (EKC and ESC) are the western boundary currents of the subarctic North Pacific and Okhotsk Sea. Variability in the EKC and ESC velocities could exert a substantial effect on ecosystems and fish stocks in the southwestern Bering Sea and Okhotsk Sea. Using satellite-derived data (sea surface heights, geostrophic current velocities, and sea surface temperatures, 2002–2020), we demonstrate that changes in zonal wind generate sea level variations on the shelf in the southwestern Bering Sea over a period of 18–29 days and with an amplitude of 5–20 cm. The ebb/flood events on the shelf lead to changes in the velocity, direction, and position of the EKC. The sea level anomalies propagate along the western Kamchatka, northern Kuril Islands and the northern and western Okhotsk Sea and result in the variability of geostrophic current velocities in the ESC zone. The strengthening (weakening) of ESC leads to an increase (a decrease) in SST in the southern part of the Okhotsk Sea by 1–3 °C. In the northwestern Okhotsk Sea, in addition to wind-induced variability, there are temporary changes in the geostrophic currents with a period of 14 days caused by fortnightly tides.

**Keywords:** satellite altimetry; sea level; geostrophic current; SST; Bering Sea; Okhotsk Sea



**Citation:** Andreev, A. Intra-Seasonal Variability of Sea Level on the Southwestern Bering Sea Shelf and Its Impact on the East Kamchatka and East Sakhalin Currents. *Remote Sens.* **2023**, *15*, 4984. <https://doi.org/10.3390/rs15204984>

Academic Editor: Chung-Ru Ho

Received: 19 September 2023

Revised: 10 October 2023

Accepted: 13 October 2023

Published: 16 October 2023



**Copyright:** © 2023 by the author. Licensee MDPI, Basel, Switzerland. This article is an open access article distributed under the terms and conditions of the Creative Commons Attribution (CC BY) license (<https://creativecommons.org/licenses/by/4.0/>).

## 1. Introduction

Wind forcing leads to anomalies in the sea surface heights (SSHs) and geostrophic current velocities. Relaxation of SSH disturbances in coastal areas can occur in the form of continental shelf waves (quasi-geostrophic gradient–eddy waves) and in the presence of a certain coastline morphometry, and stratification in the form of Kelvin waves (gravitational waves) [1]. Wind stress variations due to passage of atmospheric cyclones have been shown to cause changes in sea level and the formation of shelf waves in the northern Kuril Islands zone (North Pacific) and eastern Sakhalin shelf (southwestern Okhotsk Sea) [2,3]. The southwestern part of the Bering Sea, characterized by a wide shelf (length of 110 km in the meridional direction and 170 km in the zonal direction) and a continental slope with depth differences from 200 to 3500 m, is a favorable place for the generation of coastal trapped waves (CTWs). The propagation of CTWs impacts the currents connected to the continental slope [2,3].

Fisheries in the Bering and Okhotsk Seas are among the most productive in the world. The variations in the East Kamchatka (EKC) water transport result in changes in seawater temperature and ice coverage in the Okhotsk Sea and thereby impact on ecosystems and fish stocks, especially the pollock stock [4]. The water dynamics exert a substantial effect on the direction and rate of fish migrations in the Bering Sea [5,6]. An advection of the deep basin water on the shelf leads to the extremely high chum salmon abundance on the shelf edge of the western Bering Sea [7]. Changes in the position and strength of the EKC influence the distributions of seawater carbon dioxide partial pressure and salinity at the western boundary of the subarctic North Pacific in winter [8]. Using satellite altimetry data can significantly improve our understanding of temporal changes in SSHs and water dynamics in the East Kamchatka and East Sakhalin (ESC) currents areas. Previous studies

have mainly addressed EKC seasonal/interannual variability and mesoscale eddies in the EKC region [9,10]. The impact of intra-seasonal SSH variability on water circulation in the EKC area has not been studied. In this paper, we analyze satellite-derived data (SSHs, geostrophic current velocities, and SSTs) collected on the shelf and slope of the southwestern Bering Sea, northern Kuril Islands, and Okhotsk Sea between 2002 and 2020. First, we show the variability of SSH in the southwestern Bering Sea and SSH anomaly propagation from the Bering Sea to the Okhotsk Sea. Then, we discuss the temporal changes in the EKC and ESC velocities and SST in the southern Okhotsk Sea induced by SSH variability in the Bering Sea. Finally, we demonstrate the geostrophic current velocity oscillations with 14-day period at the boundary between the Sakhalin Bay water (Amur River influenced water) and the Okhotsk Sea water in the northwestern Okhotsk Sea.

## 2. Materials and Methods

### 2.1. Study Area

The surface circulation of the northern North Pacific consists of a counter-clockwise subarctic gyre which is connected to the cyclonic gyres in the Bering and Okhotsk Seas [11]. EKC is the western boundary current of the subarctic North Pacific (Figure 1). The EKC, flowing southward along the western Kamchatka and the northern Kuril Islands, originates from the Bering Slope Current crossing the central Bering Sea [12,13]. The EKC transport is strong in winter and relatively weak in the summer. The seasonality in the EKC flow is related to the wind stress over the northern and western Bering Sea. Strengthening of the northeastern wind in winter could increase the velocity of the EKC up to 30–40 cm/s [7]. The EKC supplies water to the Okhotsk Sea through the northern Kuril Straits [4,14–16].

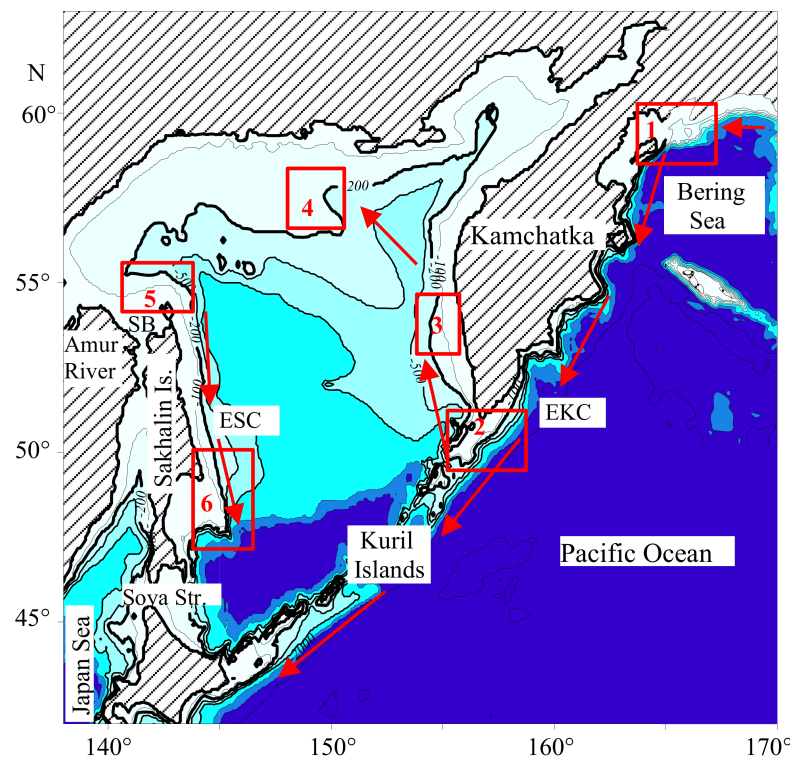


**Figure 1.** A schematic representation of the currents in the study area. EKC, East Kamchatka Current; ESC, East Sakhalin Current; Kam. Str., Kamchatka Strait; SB, Sakhalin Bay. The thick red lines and numbers indicate the areas (1—southwestern Bering Sea, 2—northern Kuril Islands zone; 3–6—northeastern, northern, northwestern, and southwestern Okhotsk Sea) where the SSHs and geostrophic current velocities were analyzed.

The ESC is the western boundary current of the Okhotsk Sea cyclonic gyre (Figure 1). It transports low-salinity surface water, influenced by the Amur River outflow, along

the eastern coast of Sakhalin Island. The geostrophic current velocities computed from shipborne hydrographic data (1950–1994) [17], mooring ADCP (Acoustic Doppler Current Profiler) data (1998–2000) [18], and satellite-derived geostrophic current velocities (1993–2012) [19,20] demonstrate that the ESC flow (similar to EKC) exhibits large seasonal variations with a maximum in fall/winter and a minimum in summer. The Soya Current water (transformed subtropical water flowing from the Japan Sea through the Soya Strait) influences the southern Okhotsk Sea. The driving force of the Soya Current is the difference in sea level between the Sea of Japan and the Okhotsk Sea [21,22].

## 2.2. Data and Methods

Our study is based on satellite-derived data on the SSHs, geostrophic current velocities, and SSTs for the period of 2002 to 2020. The SSH and geostrophic current velocity data are available on the website of the European Marine Environment Monitoring Service Copernicus (CMEMS, [https://data.marine.copernicus.eu/product/SEALEVEL\\_GLO\\_PHY\\_L4\\_MY\\_008\\_047/](https://data.marine.copernicus.eu/product/SEALEVEL_GLO_PHY_L4_MY_008_047/), accessed on 10 December 2021). These data are part of a project to process SSALTO/DUACS multi-sensor satellite altimetry data distributed by AVISO (Archiving, Validation and Interpretation of Satellite Oceanographic Data). The combined AVISO array includes corrected altimetry data from the Cryosat—2, Jason—1/2/3 series, Envisat, Topex/Poseidon, GFO—1, and ERS—1/2 satellites with a spatial resolution of  $0.25^\circ \times 0.25^\circ$  (~30 km along the longitude and 15–20 km along the latitude for the study area) and a temporal resolution of 1 day. The processing of satellite altimetry data includes corrections for instrumental errors, environmental perturbations (wet tropospheric, dry tropospheric and ionospheric effects), the ocean sea state influence (sea state bias), the tide influence (ocean tide, earth tide, and pole tide) and atmospheric pressure (combined atmospheric correction: high frequency fluctuations of the sea surface topography and inverted barometer height correction) ([https://www.aviso.altimetry.fr/fileadmin/documents/data/tools/hdbk\\_L2P\\_all\\_missions\\_except\\_S3.pdf](https://www.aviso.altimetry.fr/fileadmin/documents/data/tools/hdbk_L2P_all_missions_except_S3.pdf) (accessed on 10 December 2021)). The velocities of the geostrophic currents were computed from SSH data using the geostrophic balance equations. The accuracy of SSH satellite data is 1–2 cm at distances more than 20–40 km from the shore [23,24]. Based on the accepted SSH error value, the error of the geostrophic current velocities for the off-shore region is about 3–9 cm/s. Because of sea ice coverage from January to April [25], altimetry data collected in the northern and western Okhotsk Sea in winter/spring were excluded from the data analysis.

The SST images (spatial resolution of 1 km) were provided by the GHRSSST (Group for High-Resolution Sea Surface Temperature) (PO.DAAC–GHRSSST Level 4 MUR) (accessed on 10 June 2023). The data on wind direction and speed, as well as the geopotential of 500-mbar surface and SST anomaly (daily data) were taken from the website of the Center for Climate Diagnostics (<http://www.esrl.noaa.gov>, accessed on 5 June 2023).

## 3. Results

### 3.1. SSH Variability on the Southwestern Bering Sea

In winter, an intensification of the Aleutian depression over the northern Pacific Ocean and the Bering Sea causes northeasterly winds in the southwestern Bering Sea and an increase in the SSH at the western boundary of the Bering Sea [7]. In the cold season (December–March, 2002–2020), the southwestern Bering Sea shelf ( $59.6^\circ\text{N}$ ,  $165.1^\circ\text{E}$ ) was characterized by high SSH ( $34 \pm 8$  (std) cm,  $N = 2242$ ). In the warm season (June–September, 2002–2020), the SSH on the southwestern Bering Sea shelf was low ( $23 \pm 4$  cm,  $N = 2318$ ).

Against the background of reduced (increased) SSH in the summer (winter), SSH shows a strong intra-seasonal variability with an amplitude of 5–20 cm (Figure 2). Spectral analysis of the SSH time-series ( $59.6^\circ\text{N}$ ,  $165.1^\circ\text{E}$ ) using the Lomb–Scargle periodogram revealed statistically significant ( $p < 0.01$ ) variability of the SSH with periods of 18, 21, and 26 days in the warm season (June–September) and with periods of 18, 21, 22–24, 26, and 28–29 days in the cold season (December–March). The strongest peaks in the power spectral density corresponded to the periods of 23 and 26 days.

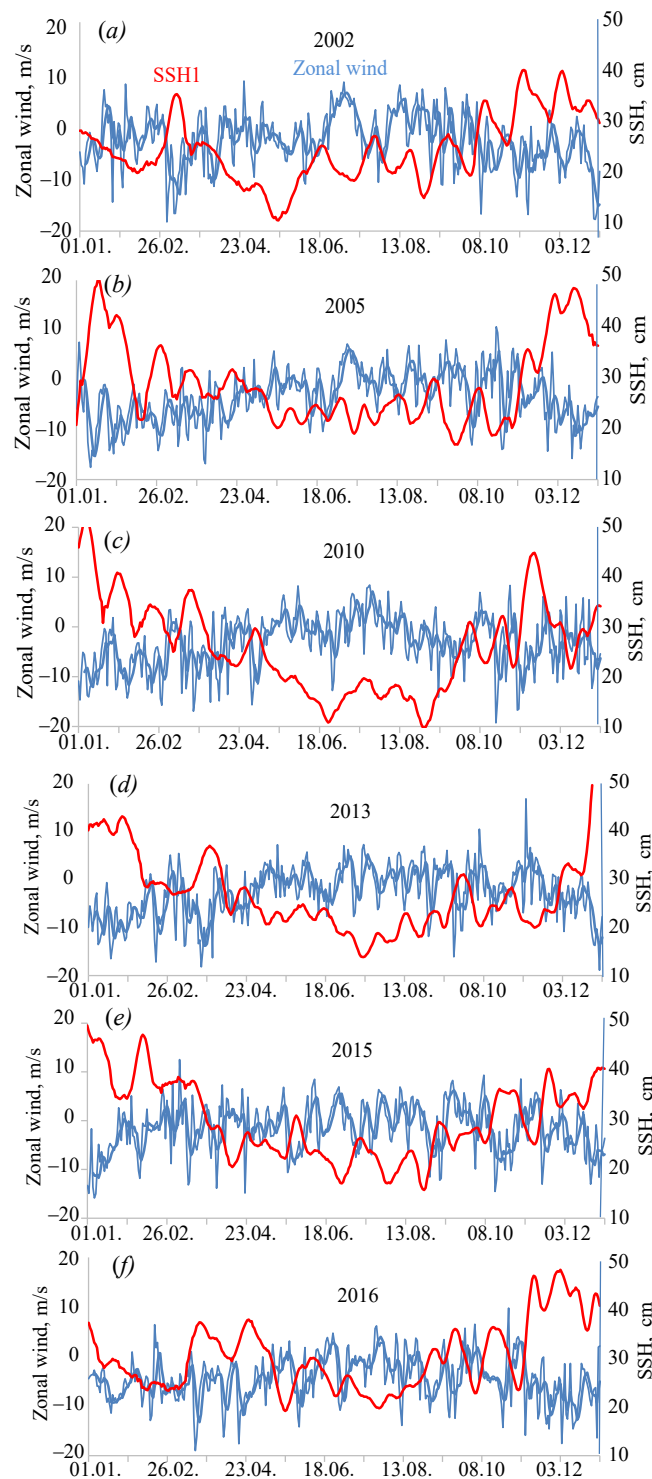


**Figure 2.** Time series of the SSH (SSH1, 59.6°N, 165.1°E) and zonal wind (60°N, 165°–172.5°E) (a–f) in the southwestern Bering Sea. The thick blue line shows the zonal wind smoothed by 5 – day running mean. Positive (negative) values of zonal wind indicate westerly (easterly) winds.

Intra-seasonal fluctuations in SSH on the shelf of the southwestern Bering Sea were related to variability in zonal wind ( $r = -0.60$ ,  $p < 0.01$ , 2002–2020, daily data). The appearance of easterly (westerly) winds (negative (positive) values of zonal wind) with speeds of 5–20 m/s was accompanied by an increase (decrease) in SSH by 5–20 cm (Figure 2). Strengthening of the westerly winds and an increase in the meridional component of the wind stress ( $\tau_x$ ), causing the Ekman transport ( $\tau_x / \rho f$ , where  $\rho$  is the density of sea water,  $f$  is

the Coriolis parameter) of shelf waters into the deep part of the Bering Sea, and a decrease in SSH (ebb events). The easterly winds, which force the water supply from the deep basin to the shelf, are accompanied by an increase in SSH (flood events).

Changes in the speed and direction of the zonal wind with a period of a few weeks (exceeding the synoptic variability with a period of 3–10 days) in the southwestern part of the Bering Sea were related to atmospheric planetary waves. The pathways of atmospheric waves in the northern North Pacific and the mechanisms of their formation are presented in [26–28]. In winter, atmospheric waves are distinguished by the distribution of the geopotential anomaly of 500-mbar surface (middle troposphere) in the form of a dipole elongated in the meridional direction with the highest amplitude over Alaska and the Bering Sea [26]. According to the results presented in [28], atmospheric waves are well manifested as an alternation of northward and southward meridional wind velocities along 40°N (“wave train”). The instability of westerly transport, heat fluxes, and energy supply from atmospheric vortices are considered to be energy sources of atmospheric wave formation [26–28]. The appearance of an atmospheric wave crest over the eastern part of the Bering Sea (19 September 2016; 22 October 2016) (Figure 3a,c) is accompanied by cyclonic atmospheric circulation in the southwestern part of the Bering Sea and easterly winds over the shelf margin (Figure 3d,f). The shift of the atmospheric wave crest to the southeastward (2 October 2016) (Figure 3b) led to westerly winds over the northwestern Bering Sea shelf (Figure 3e).

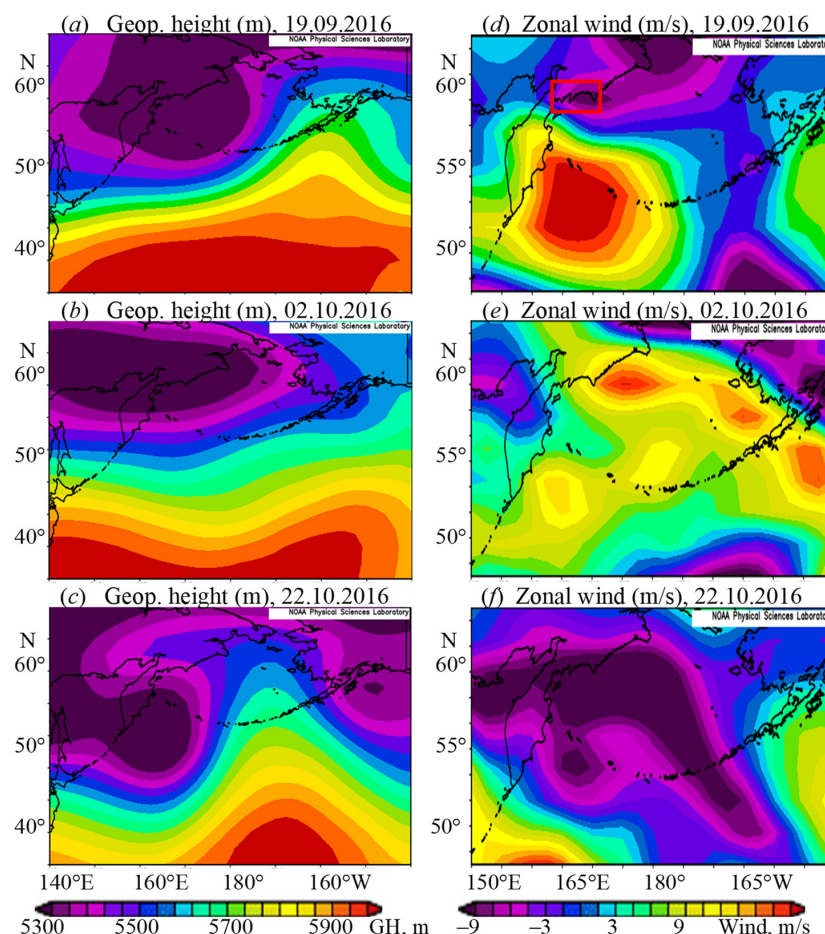


**Figure 3.** Spatial patterns of 500-mbar geopotential (m) (a–c) and zonal wind (m/s) (d–f) in the northern North Pacific, Bering, and Okhotsk Seas on 19 September, 2 October, and 22 October 2016. Solid red lines (d) mark the study area in the southwestern Bering Sea.

The distribution of SSH along the meridional shelf/deep basin section (165.1°E) during the ebb and flood events is shown in Figure 4. The strong easterly winds forced an increase in SSH by 12–14 cm in the shelf zone in from October–8 November 2002 (Figure 4a).

Westerly winds (9–24 November 2002) (Figure 2a) led to a decrease in SSH by 10 cm on the shelf and an increase in SSH by 7 cm south of the continental slope. From 10 October to 23 October 2010, an increase in easterly winds (up to 16 m/s) (Figure 2b) caused a sea level rise of 10 cm on the shelf in the southwestern part of the Bering Sea (Figure 4b). The weakening of easterly winds and the appearance of westerly winds (24 October–6 November 2010) contributed to a decrease in sea level by 10–13 cm. In March–April 2013, an increase (a decrease) in the SSH on the southwestern Bering Sea shelf was 10–12 cm (14–16 cm) (Figure 4c). In the period from 7 October to 5 November 2015, under the influence of easterly winds (Figure 2e), SSH increased from 21 to 32 cm (Figure 4d) and then decreased to 19 cm under the influence of westerly winds.

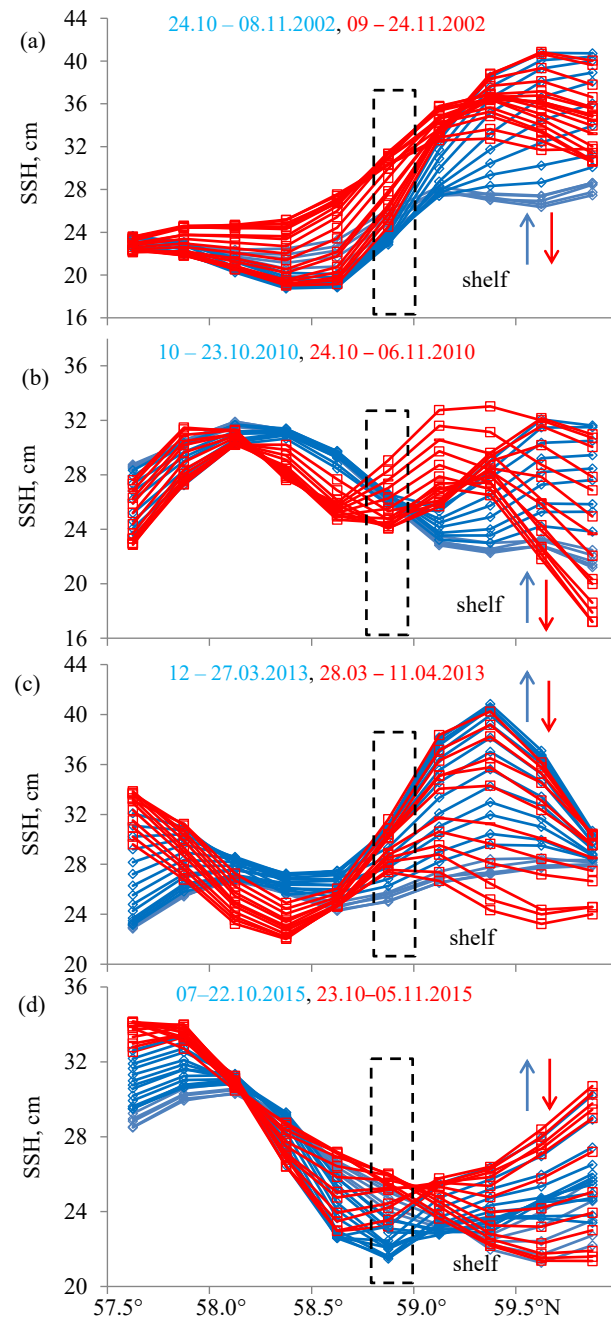


**Figure 4.** The distribution of the SSH on the meridional transect (shelf/deep basin) in the southwestern Bering Sea (165.1°E) during periods of an increase (shown by blue lines) and a decrease (shown by red lines) in the sea level on the shelf (a–d). Dotted black lines indicate the slope position. Blue and red arrows show a tendency to increase and decrease in SSH on the southwestern Bering Sea shelf.

### 3.2. Propagation of the Sea Level Anomalies

The intra-seasonal SSH oscillations generated on the shelf in the southwestern Bering Sea were observed on the shelf in the northern Kuril Islands area and the northern and western Okhotsk Sea with a time lag of 4–10 days (Figures 5 and 6). The peaks in the SSH time series observed on the southwestern Bering Sea shelf on 1 December and 16 December 2005 were accompanied by increased SSH on the shelf of the northern Kuril Islands/northeastern Okhotsk Sea on 6 and 23 December 2005 (Figure 5a), the northern Okhotsk Sea (56.1°N, 148.6–149.1°E) on 6 and 24 December 2005 (Figure 6b), and the southeastern Sakhalin on 7 and 25 December 2005 (Figure 6c). The peak in the SSH time series observed on the shelf of the northern Kuril Islands/northeastern Okhotsk Sea on 23 October 2016 (Figure 5d) and southeastern Sakhalin on 26 October 2016 (Figure 6d) was related to the peak in the SSH time series observed on the southwestern Bering Sea shelf on 17 October 2016. The sea level rise in the southwestern part of the Bering Sea from 3 October to 17 October 2016 was accompanied by an increase in the SSH on the shelf in the northern and western (eastern shelf of the Sakhalin Island) parts of the Okhotsk Sea from 9 to 25 October 2016 (Figure 6a). The amplitude of SSH intra-seasonal variability on the northeastern Okhotsk Sea shelf (SSH3, Figure 5) was approximately 5 cm lower than that on the southwestern Bering Sea shelf (SSH1, Figure 5).

The SSH anomalies (formed in the southwestern part of the Bering Sea) reached the shelf/continental slope of the northern Kuril Islands and the northeastern shelf of the Okhotsk Sea in 4–6 days (distance of about 1000 km). The average phase velocity of propagation of sea-level fluctuations in the EKC zone was 2–3 m/s. From the southwestern shelf of the Bering Sea to the southeastern shelf of Sakhalin (distance of 3500 km along the shelf edge), the sea level fluctuations propagated with an average phase velocity of 4–10 m/s.

The propagation of sea level fluctuations along the continental slope and shelf with a phase velocity of 2–10 m/s indicates the presence of CTWs (shelf and/or Kelvin waves) in the study area. The phase velocity of the barotropic Kelvin waves traveling along the slope at the shallow water gravity wave speed (50–100 m/s) is higher than that observed. In the stratified ocean, Kelvin waves (internal Kelvin waves) travel at an internal gravity wave speed (about 2 m/s in the study area) [29]. Whether coastal trapped waves belong to shelf waves or internal Kelvin waves is determined by the stratification parameter (Burger number;  $S = Rd/L$ , where  $Rd$  is the Rossby baroclinic deformation radius,  $L$  is the shelf width) [1,2]. For the study area,  $Rd$  is 20 km [29]. The phase velocity of the shelf waves is determined by the Coriolis parameter and the shelf width ( $f \cdot L$ ) [1,2]. Favorable conditions for the propagation of shelf waves are observed in the southwestern part of the Bering Sea (shelf width is about 110 km), the zone of the northern Kuril Islands (shelf width is about 75 km), the northern (shelf width is about 200–300 km) and western (shelf width is about 70–200 km) parts of the Okhotsk Sea.

The wide shelf of the western and northern Okhotsk Sea provides a high phase velocity for the shelf waves and leads to a small phase shift (1–3 days) in the SSH anomaly propagation between the northeastern and southwestern Okhotsk Sea shelves. The eastern coast of the Kamchatka is characterized by a narrow shelf (~30 km). For this region, the Burger number is close to unity. Intra-seasonal level anomalies formed in the southwestern part of the Bering Sea can enter the zone of the northern Kuril Islands in the form of mixed (hybrid) waves. The narrow shelf, the presence of bays and capes limit the use of satellite altimetry data to study the propagation of CTWs along the eastern Kamchatka.

SSH fluctuations in the area of the Kuril Islands were influenced by the meridional wind. The southerly winds (positive values of the meridional wind) decreased the SSH on the northern Kuril Islands shelf and, as a result, changed the SSH signal coming from the Bering Sea (7–13 November 2002) (Figure 5a). Northerly winds generated positive SSH anomalies on the shelf of the northern Kuril Islands (19–26 November 2002), which then supplied to the northeastern Okhotsk Sea. The atmospheric waves over the North Pacific generate intra-seasonal quasiperiodic variability in the zonal wind over the southwestern part of the Bering Sea (Figure 2), but do not lead to quasiperiodic variations in the meridional wind in the area of the northern Kuril Islands. Our results show that on time scales

exceeding the synoptic one, the intra-seasonal sea level fluctuations in the northern Kuril Islands could be due to SSH anomaly propagation from the southwestern Bering Sea.

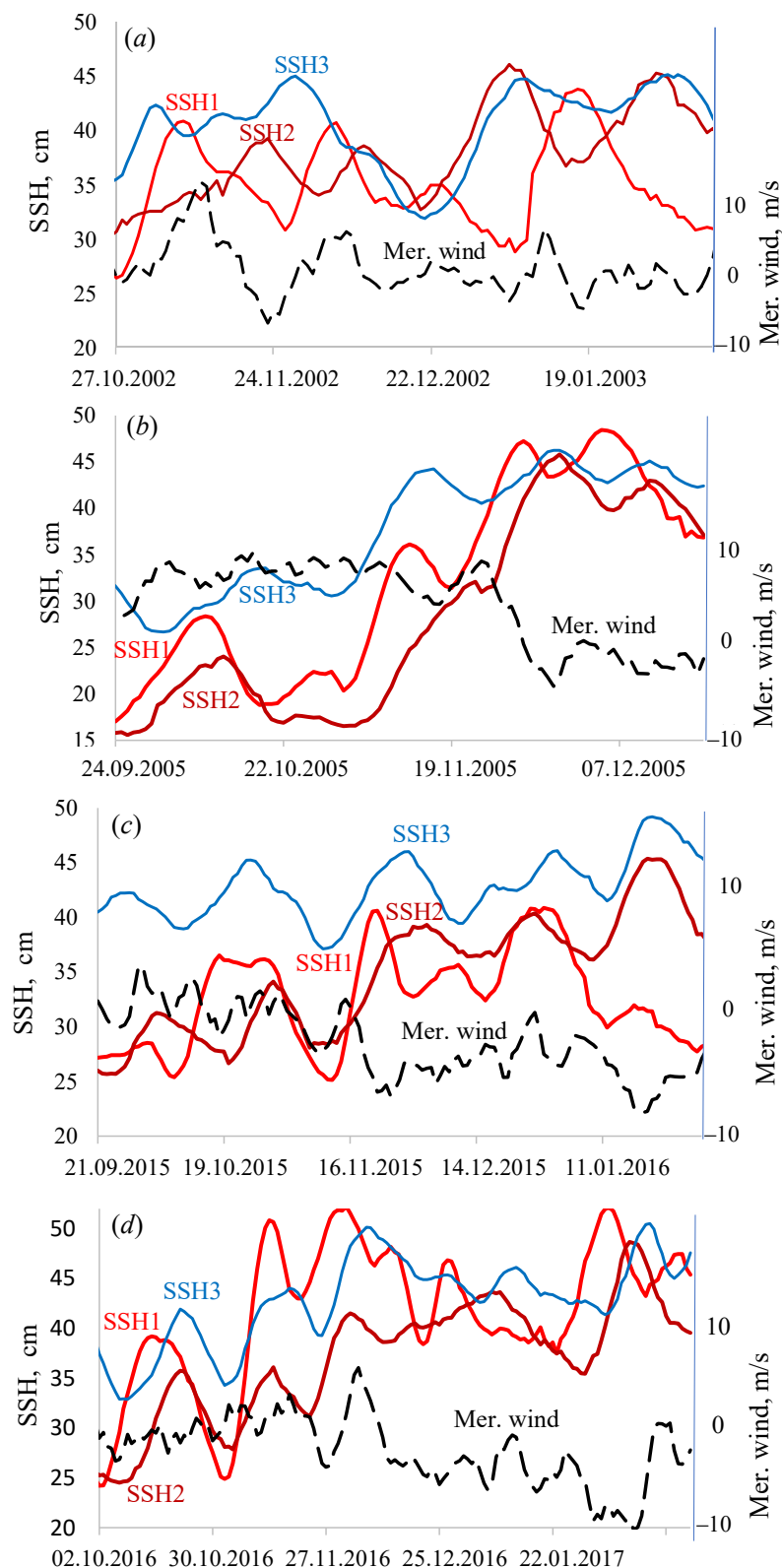


**Figure 5.** Time series of the sea level in the southwestern Bering Sea (SSH1, 59.6°N, 165.1°E), northern Kuril Islands area (SSH2, 50.4°N, 165.1°E), and northeastern Okhotsk Sea (SSH3, 53.9°N, 155.4°E) and time series of the meridional wind over the northern Kuril Islands area (50°N, 157.5°E) (a–d).

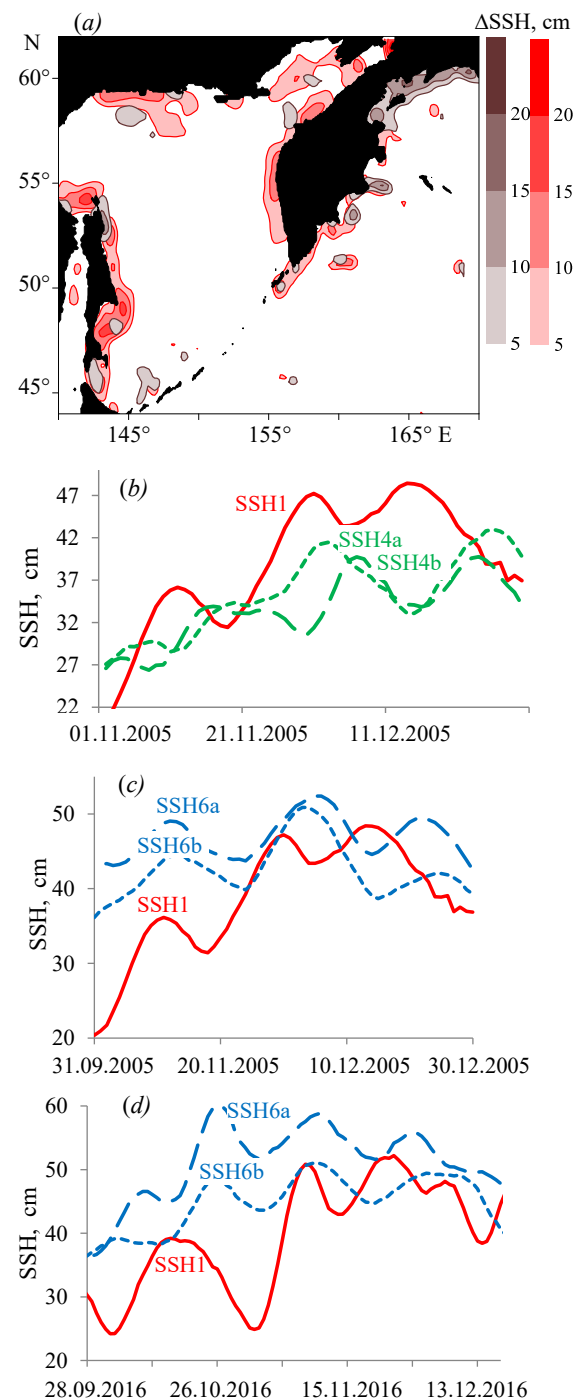


**Figure 6.** The distribution of the difference in SSH between 17 October 2016 and 3 October 2016 (shown by brown color) and the difference in SSH between 25 October 2016 and 9 October 2016 (shown by red color) (a); time series of the of the sea level on the shelf in the southwestern Bering Sea (SSH1, 59.6°N, 165.1°E), the northern Okhotsk Sea (SSH4a, central part of the shelf: 57.6°N, 148.6°–149.1°E; SSH4b, shelf edge: 56.1°N, 148.6°–149.1°E) in 2005 (b), and the southwestern Okhotsk Sea (SSH6a, shelf edge: 48.4°N, 145.1°E; SSH6b, central part of the shelf: 48.4°N, 144.4°E) in 2005 and 2016 (c,d).

### 3.3. Intra-Seasonal Variability of EKC and ESC Velocities

Intra-seasonal sea level variations in the zone of the shelf and the continental slope in the southwestern part of the Bering Sea lead to changes in direction and velocity along the slope EKC. During the periods of January–April 2011, November–December 2011,

January–March 2015 and December 2015, the main jet of the EKC was directed to the west and was characterized by velocities of 15–30 cm/s (Figure 7). The decrease in SSH on the shelf led to a weakening of the EKC and/or a change in its direction from westward to eastward. During these periods, an eastward flow of water was observed in the shelf zone (59.2°–59.9°N) with current velocities of 10–20 cm/s. The increase in SSH on the shelf caused by flood/ebb events and an increase in the sea level difference between the shelf and the deep-water basin led to an increase in the westward EKC (the current velocity increased from 5–10 cm/s to 15–30 cm/s). In the warm season (June–September), the EKC was directed eastward and was characterized by velocities of 2–15 cm/s. The increase (decrease) in SSH on the shelf of the southwestern part of the Bering Sea led to a weakening (strengthening) of the water flow directed along the continental slope.

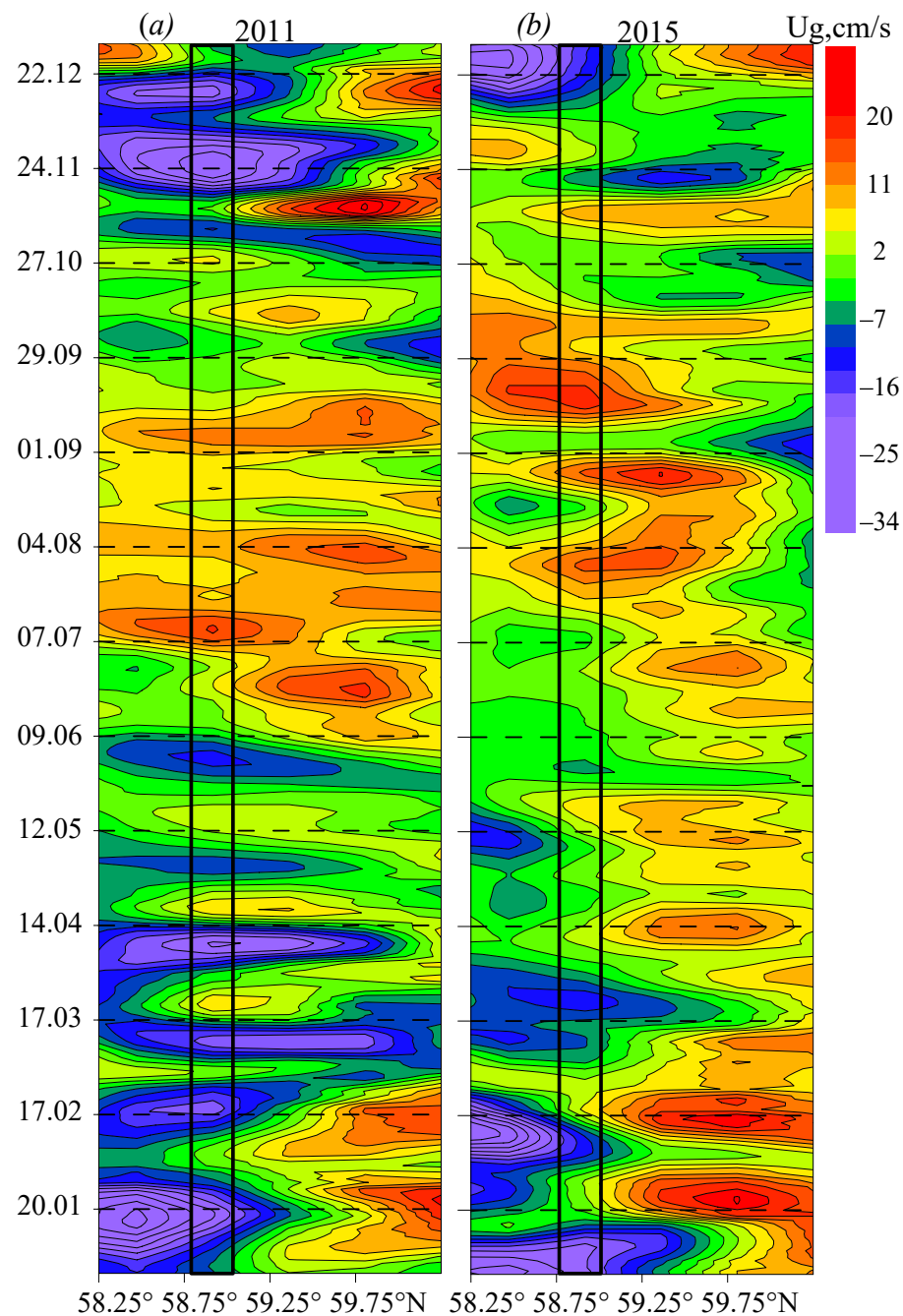


**Figure 7.** Hovmöller diagram (time vs. latitude, 165.1°E) for zonal geostrophic velocity in the southwestern Bering Sea in 2011 (a) and 2015 (b). Solid black lines indicate the slope position.

Intra-seasonal SSH changes on the shelf and slope cause variations in the EKC velocity in the zone of the northern Kuril Islands. Figure 8 shows the intra-seasonal changes in the SSH and the meridional geostrophic velocities on the shelf/deep basin section (along 50.1°N) from October–December 2012. The SSH fluctuations on the shelf and slope with a period of approximately 28 days (Figure 8) resulted in strengthening/weakening of the EKC stream (directed southward along the slope) and shifted the location of the EKC stream. The velocities of the geostrophic current varied from 10 to 45 cm/s. An intensification of the EKC (southward flow along the slope) was accompanied by a northward-directed geostrophic flow (with velocities of 5–25 cm/s) in the shelf zone (<156.4°E).

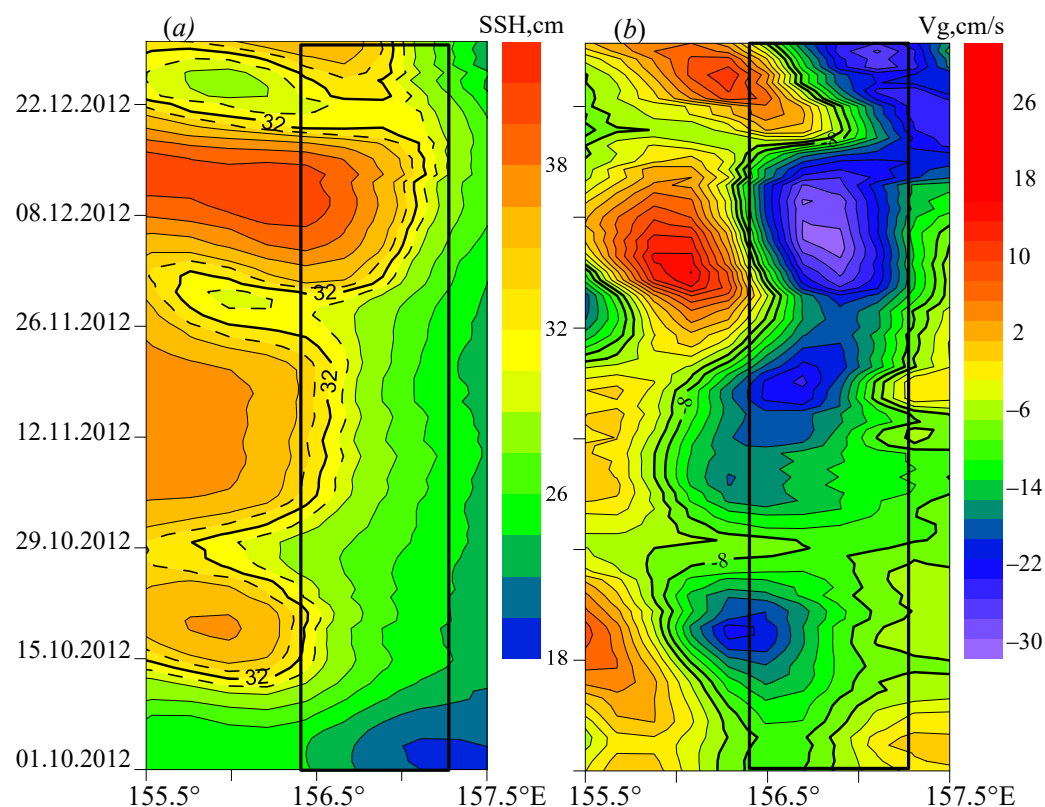


**Figure 8.** Hovmöller diagram (time vs. longitude, 50.1°N) for the SSH (a) and meridional geostrophic velocity (b) in the northern Kuril Islands area in 2012. Solid black lines (a,b) indicate the slope position.

Intra-seasonal SSH variability on the southeastern Sakhalin shelf leads to temporal changes in ESC velocities. The SSH rise on the shelf (25 October 2016 and 18 November 2016) was accompanied by an increase in the ESC velocity and a decrease in the inflow of the Soya Current water from the Japan Sea to the Okhotsk Sea (Figure 9a,c). The SSH decrease on the southeastern shelf of Sakhalin (18 November 2016) led to the weakening of the ESC flow and increased inflow of Soya waters into the Okhotsk Sea (Figure 9b). The weakening (strengthening) of the inflow of Soya waters could be due to an increase (a decrease) of SSH on the shelf of the southwestern Okhotsk Sea and, as a result, a decrease (an increase) in the sea level difference between the northeastern Japan Sea and the southwestern Okhotsk Sea. The intra-seasonal variability of the SSH on the Sakhalin shelf (due to supply of the sea level anomalies from the southwestern Bering Sea) resulted in changes in the EKC velocity at 15–30 cm/s (Figure 9d–f).

In fall, the Soya Current waters are a source of heat for the southern Okhotsk Sea (Figure 10a,b). The strengthening (weakening) of the ESC, due to the supply of positive (negative) SSH anomalies from the southwestern part of the Bering Sea, leads to an increase (a decrease) in SST in the southern part of the Okhotsk Sea by 1–3 °C (Figure 10c–e). The correlation coefficient between SSH changes on the shelf of the southwestern Bering Sea

and SST anomalies in the southern Okhotsk Sea (September–December, daily data) is  $-0.57$ – $-0.78$  ( $p < 0.01$ ).

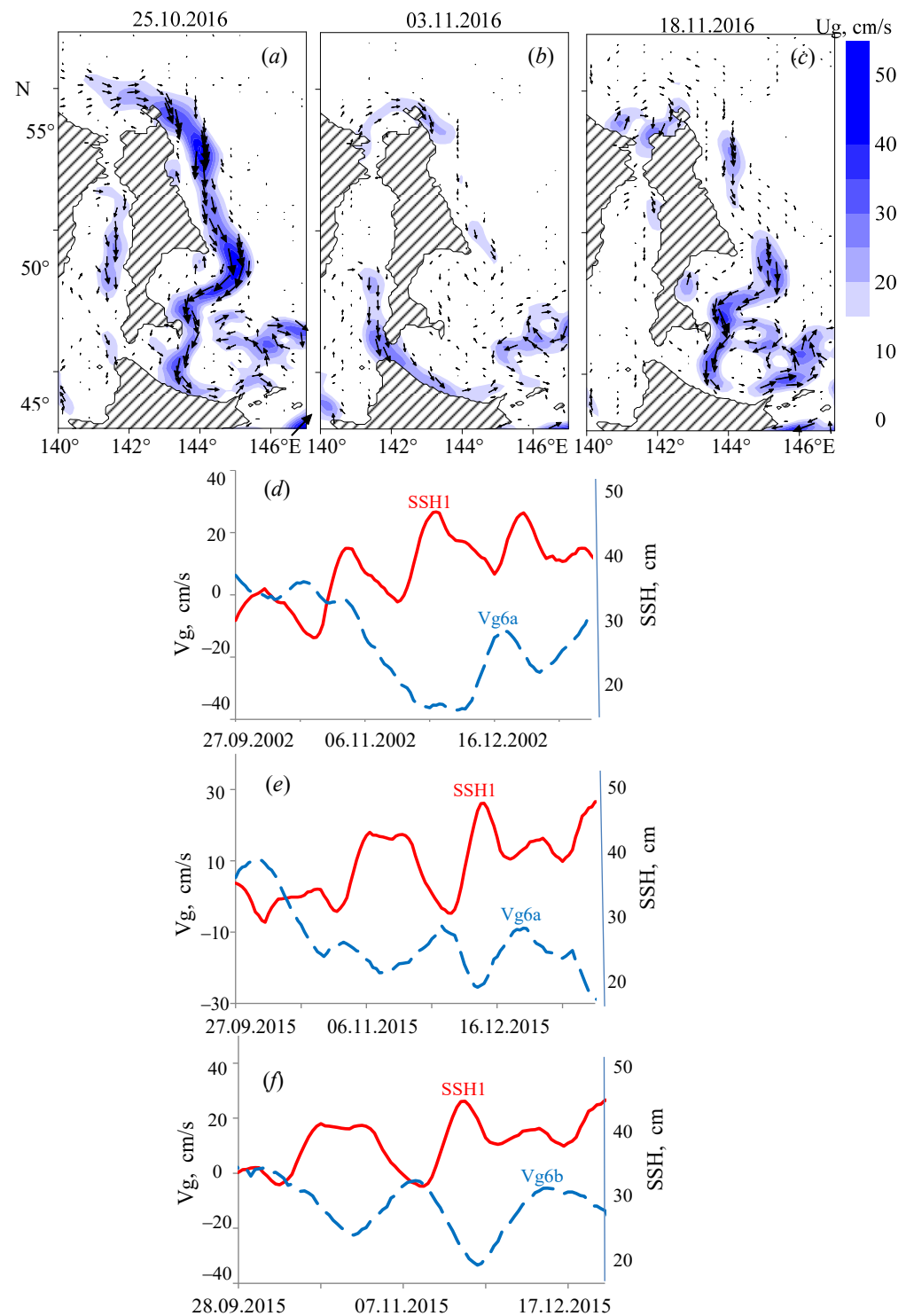


**Figure 9.** Geostrophic velocity fields in the western Okhotsk Sea and northern Japan Sea during periods of increased SSH (25 October and 18 November 2016) (a,c) and decreased SSH (3 November 2016) (b) on the southwestern Okhotsk Sea shelf (see Figure 6c); temporal changes in the sea level in the southwestern Bering Sea (SSH1, 59.6°N, 165.1°E) and meridional velocities in the ESC area (Vg6a, 48.9°N, 145.1°E; Vg6b, 45.6°N, 143.6°E) in 2005 and 2016 (d–f).

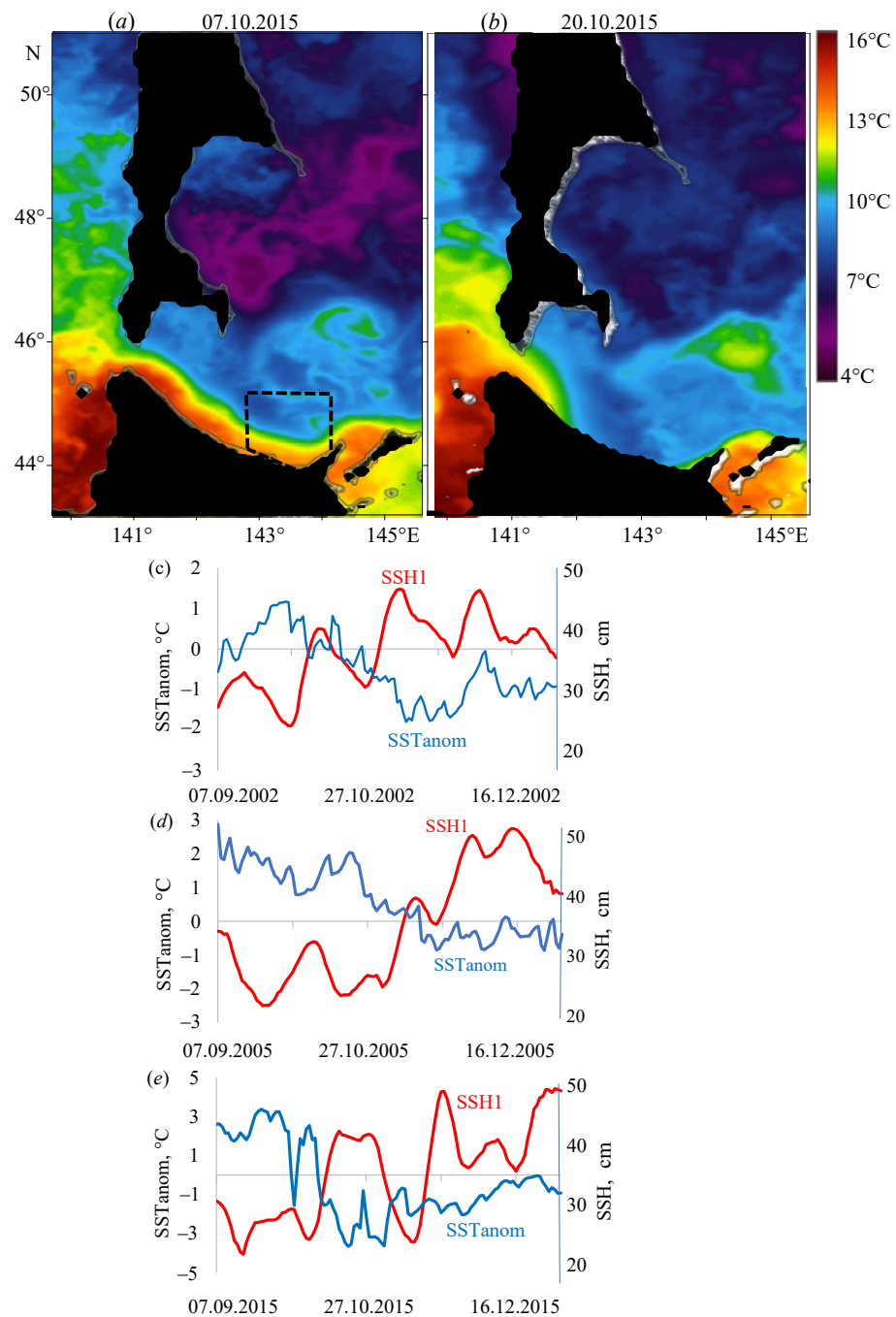


**Figure 10.** The distribution of the SST in the southwestern Okhotsk Sea on 7 and 20 October 2015 (a,b) and the temporal changes in the sea level in the southwestern Bering Sea (SSH1, 59.6°N, 165.1°E) and the SST anomaly in the southern Okhotsk Sea (c–e). The dotted black lines (a) indicate the area where the SSTs were analyzed.

### 3.4. Intra-Seasonal Variability of Geostrophic Velocities in the Northwestern Part of the Okhotsk Sea

The ESC originates in the northwestern Okhotsk Sea (Figure 9a–c). This area is characterized by a significant gradient of SSH at the boundary between Sakhalin Bay and the open Okhotsk Sea [30]. The Amur River outflow (about 390 km<sup>3</sup> per year) supplies to the Amur Estuary and Sakhalin Bay and then to the Okhotsk Sea. Approximately 87% of the annual Amur River discharge falls during the warm part of year (from May to October) [31].

In fall, the difference in SSH and SST between the Sakhalin Bay waters and the northwestern Okhotsk Sea waters reached 10–12 cm and 4–6 °C (Figure 11a,c,d,f). A significant meridional gradient of SSH at the edge of Sakhalin Bay waters in the northwestern Okhotsk

Sea leads to the appearance of an eastwardly directed current with velocities of 15–35 cm/s. In this region, in addition to intra-seasonal SSH changes due to winds, there are temporary changes in SSH and geostrophic currents with a period of 14 days caused by fortnightly tides. The area of the Okhotsk Sea off the northern Sakhalin Island is characterized by diurnal tides with a pronounced 2-week variability due to the superposition of two main diurnal tidal waves, K1 (lunar–solar with a period of 23.93 h) and O1 (principal lunar with a period of 25.82 h) [32]. Figure 12a demonstrates that during the periods of September–October 2005 and September–October 2011, high (low) velocities in the study area were observed during the periods of increased (decreased) fortnightly tides with a lag of 4–5 days (each year the phase of maximum/minimum fortnightly tide shifts by 3.5 days; the periods of enhanced fortnightly tides in 2011 correspond to the periods of low tides in 2005). An increase in the zonal velocities in the study area was due to a higher (lower) difference in SSH between Sakhalin Bay and the northwestern Okhotsk Sea during the periods of enhanced fortnightly tides (17 September and 1 October 2005) (Figure 11a,c). In November, due to decreased Amur River discharge (and low difference in the SSH between Sakhalin Bay and the northwestern Okhotsk Sea), the SSH in the study area was influenced by sea level anomalies supplied from the Bering Sea and Kuril Islands (Figure 12b). From December to June, the study of the SSH and geostrophic current variability using altimetry data in the Sakhalin Bay zone could not be conducted because of heavy ice conditions in this area.

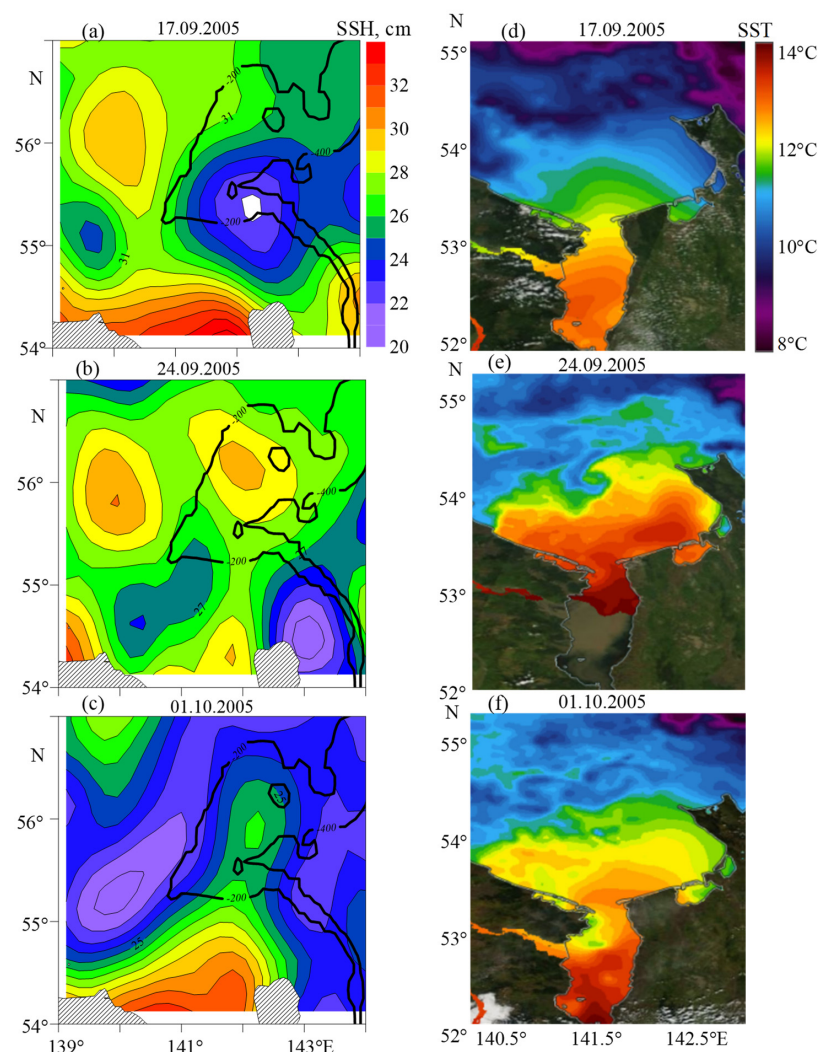


**Figure 11.** Distribution of the SST and SSH in the northwestern Okhotsk Sea during periods of increased (17 September and 1 October 2005) (a,c,d,f) and decreased (24 September 2005) (b,e) fortnightly tides.

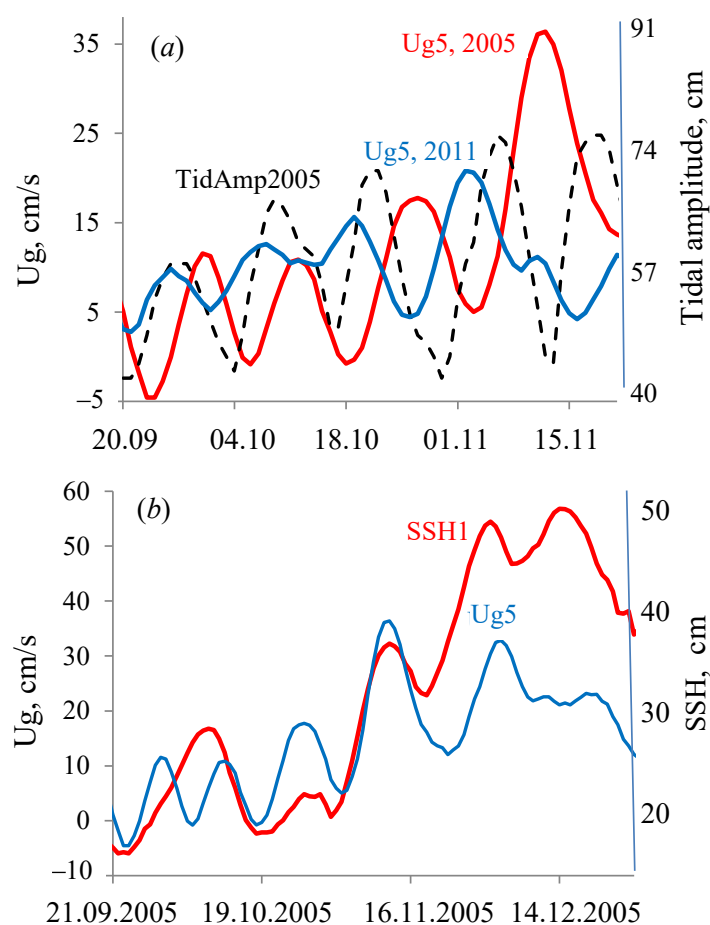


**Figure 12.** Temporal changes in the tidal amplitude (Kuegda Bay, 54.19°N, 142.36°E) and zonal velocity (Ug5, 48.4°N, 144°–145°E) in the northwestern Okhotsk Sea in 2005 and 2011 (a) and temporal changes in the sea level in the southwestern Bering Sea (SSH1, 59.6°N, 165.1°E) and zonal velocity in the northwestern Okhotsk Sea (Ug5, 48.4°N, 144°–145°E) in 2005 (b).

#### 4. Discussion

Based on meteorological and satellite data, we estimated the temporal characteristics of flood/ebb events on the southwestern Bering Sea shelf and slope in response to variability of wind forcing. Changes in zonal wind generate sea level variations on the shelf in the southwestern Bering Sea over a period of 18–29 days and with an amplitude of 5–20 cm. The intra-seasonal sea level variations in the zone of the shelf and the continental slope in the southwestern part of the Bering Sea lead to changes in the direction and velocity of the EKC connected to the slope. An increase in the EKC advection in winter leads to the increased SST and decreased ice area in the Okhotsk Sea [4]. Therefore, an intensification/deceleration of the EKC because of intra-seasonal variability in the SSH could influence the SST and ice conditions in the Okhotsk Sea.

Changes in the speed and direction of the zonal wind over a period of a few weeks in the southwestern part of the Bering Sea were related to atmospheric planetary waves. Ongoing climate change could impact the amplitude and periodicity of atmospheric planetary waves in the northern North Pacific and Bering Sea, thereby influences the intra-seasonal variability of SSH. The possible influence of climate change on the frequency and duration of flood/ebb events in the southwestern Bering Sea shelf zone requires specific research and is a subject of future work.

A significant increase (decrease) in seawater carbon dioxide partial pressure ( $p\text{CO}_{2\text{sw}}$ ) and salinity in the northern Kuril Islands zone in winter is connected to the coastal (off shore) branch of the EKC [8]. Therefore, intra-seasonal changes in the position and strength

of the EKC could impact the distributions of  $p\text{CO}_2\text{sw}$  and salinity at the western boundary of the subarctic North Pacific.

Intra-seasonal SSH oscillations generated on the shelf in the southwestern Bering Sea were observed on the shelf in the northern Kuril Islands area and the northern and western Okhotsk Sea with a time lag of 4–10 days. The propagation of sea level fluctuations along the continental slope and shelf with a phase velocity of 2–10 m/s indicates the presence of CTWs in the study area. However, a detailed study of the influence of wind-driven flood/ebb events on the Bering Sea shelf on the SSH anomaly dynamics in the Bering and Okhotsk seas requires numerical modeling.

The seasonal and interannual variability in ESC transport could be explained by temporal changes in wind stress in the Okhotsk Sea [18,33,34]. Current measurements (August 1998–September 1999, mooring ADCPs) in the shelf and slope regions of eastern Sakhalin Island demonstrated intra-seasonal variability of the ESC velocities with periods of 4–7, 8–13, and 16–64 days [3]. The authors related the variability of ESC and CTW formations to the wind stress over the northern and western shelves of the Okhotsk Sea and the wind stress curl in the central part of the Okhotsk Sea. The coastal tide gauge data (monthly data) [35] and satellite altimetry data (recent study) show that in addition to the temporal variability of the SSH and geostrophic currents induced by local winds, the SSH anomalies supplied from the southwestern Bering Sea could also generate the intra-seasonal variability of the ESC. In fall, the strengthening (weakening) of ESC, caused by positive (negative) SSH anomalies, leads to an increase (a decrease) in SST in the southern part of the Okhotsk Sea by 1–3 °C.

At the boundary between Sakhalin Bay and the northwestern Okhotsk Sea, in addition to wind-induced variability, there are temporary changes in the geostrophic currents with a period of 14 days caused by fortnightly tides. The fortnightly tides influence the SSH and SST in this area. The existence of 14-day variability should be considered in the analysis and discussion of satellite and ship-derived data collected in the northwestern Okhotsk Sea.

## 5. Conclusions

Using satellite-derived data (sea surface heights, geostrophic current velocities, and sea surface temperatures, 2002–2020), we demonstrate that changes in zonal wind generate sea level variations on the shelf in the southwestern Bering Sea with a period of 18–29 days and amplitude of 5–20 cm. The ebb/flood events on the shelf lead to changes in the velocity, direction, and position of the East Kamchatka Current. The sea level anomalies propagate along the western Kamchatka, northern Kuril Islands, northern and western Okhotsk Sea and result in the variability of geostrophic current velocities in the East Sakhalin Current zone. In fall, the strengthening (weakening) of ESC, caused by positive (negative) SSH anomalies, leads to an increase (a decrease) in SST in the southern part of the Okhotsk Sea by 1–3 °C. At the boundary between Sakhalin Bay and the northwestern Okhotsk Sea, in addition to wind-induced SSH variability, there are temporary changes in SSH and geostrophic currents with a period of 14 days, caused by fortnightly tides.

**Funding:** This study was carried out within the framework of the POI FEB RAS project (0211-2021-0014) and Russian Science Foundation project (№ 21-17-00027).

**Data Availability Statement:** Publicly available datasets were analyzed in this study.

**Conflicts of Interest:** The author declares no conflict of interest.

## References

1. Gill, A.E. *Atmosphere–Ocean Dynamics*; Academic Press: Cambridge, MA, USA, 1982; 662p. [[CrossRef](#)]
2. Efimov, V.V.; Kulikov, E.A.; Rabinovich, A.B.; Fajn, I.V. *Waves in the Border Zones of the World Ocean*; Gidrometeoizdat: Leningrad, Russia, 1985; 280p. (In Russian)
3. Mizuta, G.; Ohshima, K.I.; Fukamachi, Y.; Wakatsuchi, M. The variability of the East Sakhalin Current induced by winds over the continental shelf and slope. *Mar. Res.* **2005**, *63*, 1017–1039. [[CrossRef](#)]

4. Prants, S.V.; Andreev, A.G.; Budyansky, M.V.; Uleysky, M.Y. Impact of the Alaskan Stream flow on surface water dynamics, temperature, ice extent, plankton biomass, and walleye pollock stocks in the eastern Okhotsk Sea. *J. Mar. Syst.* **2015**, *151*, 47–56. [[CrossRef](#)]
5. Khen, G.V.; Basyuk, E.O.; Vanin, N.S.; Matveev, V.I. Hydrography and biological resources in the western Bering Sea. *Deep-Sea Res. II* **2013**, *94*, 106–120. [[CrossRef](#)]
6. Khen, G.V.; Zavolokin, A.V. The change in water circulation and its implication for the distribution and abundance of salmon in the western Bering Sea in the early 21st century. *Russ. J. Mar. Biol.* **2015**, *41*, 22–41. [[CrossRef](#)]
7. Andreev, A.G.; Budyansky, M.V.; Khen, G.V.; Uleysky, M.Y. Water dynamics in the western Bering Sea and its impact on chlorophyll a concentration. *Ocean Dyn.* **2020**, *70*, 593–602. [[CrossRef](#)]
8. Andreev, A.G.; Pipko, I.I. Water circulation, temperature, salinity, and pCO<sub>2</sub> distribution in the surface layer of the East-Kamchatka Current. *J. Mar. Sci. Eng.* **2022**, *10*, 1787. [[CrossRef](#)]
9. Isoguchi, O.; Kawamura, H. Seasonal to interannual variations of the western boundary current of the subarctic North Pacific by a combination of the altimeter and tide gauge sea levels. *J. Geophys. Res.* **2006**, *111*, C04013. [[CrossRef](#)]
10. Prants, S.V.; Budyansky, M.V.; Lobanov, V.B.; Sergeev, A.F.; Uleysky, M.Y. Observation and Lagrangian Analysis of Quasi-Stationary Kamchatka Trench Eddies. *J. Geophys. Res.* **2020**, *125*, e2020JC016187. [[CrossRef](#)]
11. Favorite, F. Flow into the Bering Sea through Aleutian Island passes. In *Oceanography of the Bering Sea with Emphasis on Renewable Resources*; University of Alaska: Fairbanks, AK, USA, 1974; pp. 3–37.
12. Stabeno, P.J.; Reed, R.K. Circulation in the Bering Sea basin by satellite-tracked drifters. *J. Phys. Oceanogr.* **1994**, *24*, 848–854. [[CrossRef](#)]
13. Panteleev, G.; Yaremchuk, M.; Luchin, V.; Nechaev, D.; Kukuchi, T. Variability of the Bering Sea circulation in the period 1992–2010. *J. Oceanogr.* **2012**, *68*, 485–496. [[CrossRef](#)]
14. Talley, L.D.; Nagata, Y. *The Okhotsk Sea and Oyashio Region*; North Pacific Marine Science Organization (PICES): Patricia Bay, BC, Canada, 1995; pp. 2–50.
15. Ohshima, K.I.; Nakanowatari, T.; Riser, S.; Wakatsuchi, M. Seasonal variation in the in- and outflow of the Okhotsk Sea with the North Pacific. *Deep Sea Res. II* **2010**, *57*, 1247–1256. [[CrossRef](#)]
16. Kida, S.; Qiu, B. An exchange flow between the Okhotsk Sea and the North Pacific driven by the East Kamchatka Current. *J. Geophys. Res.* **2013**, *118*, 6747–6758. [[CrossRef](#)]
17. Pishchalnik, V.M.; Arhipkin, V.S. Seasonal variations of the circulation on Sakhalin shelf. In *Hydrometeorological and Ecological Conditions of the Far-Eastern Seas: Marine Environmental Impact Assessment*; FERHRI Special Issue 2; Dalnauka: Vladivostok, Russia, 1999; pp. 84–95. (In Russian)
18. Mizuta, G.; Fukamachi, Y.; Ohshima, K.I.; Wakatsuchi, M. Structure and seasonal variability of the East Sakhalin Current. *J. Phys. Oceanogr.* **2003**, *33*, 2430–2445. [[CrossRef](#)]
19. Ebuchi, N. Seasonal and interannual variations in the East Sakhalin current revealed by TOPEX/POSEIDON altimeter data. *J. Oceanogr.* **2006**, *62*, 171–183. [[CrossRef](#)]
20. Prants, S.V.; Andreev, A.G.; Uleysky, M.Y.; Budyansky, M.V. Mesoscale circulation along the Sakhalin Island eastern coast. *Ocean Dyn.* **2017**, *67*, 345–356. [[CrossRef](#)]
21. Matsuyama, M.; Wadaka, M.; Abe, T.; Aota, M.; Koike, Y. Current structure and volume transport of the Soya Warm Current in summer. *J. Oceanogr.* **2006**, *62*, 197–205. [[CrossRef](#)]
22. Ohshima, K.I.; Simizu, D.; Ebuchi, N.; Morishima, S.; Kashiwase, H. Volume, heat, and salt transports through the Soya Strait and their seasonal and interannual variations. *J. Phys. Oceanogr.* **2017**, *47*, 999–1019. [[CrossRef](#)]
23. Ablain, M.; Cazenave, A.; Larnicol, G.; Balmaseda, M.; Cipollini, P.; Faugère, Y.; Fernandes, M.J.; Henry, O.; Johannessen, J.A.; Knudsen, P.; et al. Improved sea level record over the satellite altimetry era (1993–2010) from the Climate Change Initiative project. *Ocean Sci.* **2015**, *11*, 67–82. [[CrossRef](#)]
24. Ablain, M.; Picot, N. DUACS DT2014: The new multi-mission altimeter dataset reprocessed over 20 years. *Ocean Sci.* **2016**, *12*, 1067–1090. [[CrossRef](#)]
25. Minervin, I.G.; Romanyuk, V.A.; Pishchal'nik, V.M.; Truskov, P.A.; Pokrashenko, S.A. Zoning the ice cover of the Sea of Okhotsk and the Sea of Japan. *Her. Russ. Acad. Sci.* **2015**, *85*, 132–139. [[CrossRef](#)]
26. Kushnir, Y. Retrograding wintertime low-frequency disturbances over the North Pacific Ocean. *J. Atmos. Sci.* **1987**, *44*, 2727–2742. [[CrossRef](#)]
27. Alexander, M.A.; Scott, J.D. Surface flux variability over the North Pacific and North Atlantic Oceans. *J. Clim.* **1997**, *10*, 2963–2978. [[CrossRef](#)]
28. Du, L.; Lu, R. Wave trains of 10–30-day meridional wind variations over the North Pacific during summer. *J. Clim.* **2021**, *34*, 9267–9277. [[CrossRef](#)]
29. Chelton, D.B.; De Szoeke, R.A.; Schlax, M.G.; El Naggar, K.; Siwertz, N. Geographical variability of the first-baroclinic Rossby radius of deformation. *J. Phys. Oceanogr.* **1998**, *28*, 433–460. [[CrossRef](#)]
30. Andreev, A.G. The distribution of the desalinated waters of the Amur estuary in the Okhotsk Sea according to satellite observations. *Izv. Atmos. Ocean. Phys.* **2019**, *55*, 1160–1165. [[CrossRef](#)]
31. Zhabin, I.A.; Abrosimova, A.A.; Dubina, V.A. Influence of the Amur River runoff on the hydrological conditions of the Amur Liman and Sakhalin Bay (Sea of Okhotsk) during the spring-summer flood. *Russ. Meteorol. Hydrol.* **2010**, *35*, 295–300. [[CrossRef](#)]

32. Gluhovskiy, B.H.; Goptarev, N.P.; Terziev, F.S. Hydrometeorology and hydrochemistry of the seas. In *Okhotsk Sea; Hydrometeorological Conditions*; Gidrometeoizdat: Saint Petersburg, Russia, 1998; 342p. (In Russian)
33. Ohshima, K.I.; Simizu, D.; Itoh, M.; Mizuta, G.; Fukamachi, Y.; Riser, S.C.; Wakatsuchi, M. Sverdrup balance and the cyclonic gyre in the Sea of Okhotsk. *J. Phys. Oceanogr.* **2004**, *34*, 513–525. [[CrossRef](#)]
34. Simizu, D.; Ohshima, K.I. A model simulation on the circulation in the Sea of Okhotsk and the East Sakhalin Current. *J. Geophys. Res.* **2006**, *111*, C05016. [[CrossRef](#)]
35. Nakanowatari, T.; Ohshima, K.I. Coherent sea level variation in and around the Sea of Okhotsk. *Prog. Oceanogr.* **2014**, *126*, 58–70. [[CrossRef](#)]

**Disclaimer/Publisher’s Note:** The statements, opinions and data contained in all publications are solely those of the individual author(s) and contributor(s) and not of MDPI and/or the editor(s). MDPI and/or the editor(s) disclaim responsibility for any injury to people or property resulting from any ideas, methods, instructions or products referred to in the content.